PROCEEDINGS OF SCIENCE

Search for $H^{\pm}$ and $H^{\pm\pm}$ to other states than $\tau_{\text{had}}\nu$ in ATLAS

Catrin Bernius*
On behalf of the ATLAS collaboration
Louisiana Tech University
E-mail: Catrin.Bernius@cern.ch

Results of searches for charged Higgs bosons based on data from pp collisions at $\sqrt{s} = 7$ TeV, collected with the ATLAS experiment at the LHC are presented. Three analyses with the final states $\tau_{\text{lep}}\nu$ + lepton, $\tau_{\text{lep}}\nu$ + jets and $c\bar{s}$ + lepton are discussed, as well as the search for a doubly charged Higgs boson through the anomalous production of like-sign muon pairs.

Prospects for Charged Higgs Discovery at Colliders - Charged 2012,
October 8-11, 2012
Uppsala University, Sweden

*Speaker.

1. Introduction

The results of four searches for charged and doubly charged Higgs bosons presented in this paper are based on data from pp collisions at $\sqrt{s} = 7$ TeV, collected in 2011 with the ATLAS experiment [1] at the LHC. In Section 2, the three searches for charged Higgs bosons in $t\bar{t}$ events with the final states $H^+ \to \tau_{\text{lep}}\nu$ + lepton (Section 2.1), $H^+ \to \tau_{\text{lep}}\nu$ + jets (Section 2.2) and $H^+ \to c\bar{s}$ + lepton (Section 2.3) are described. The search for a doubly charged Higgs boson is described in Section 3.

2. Charged Higgs searches

Charged Higgs bosons ($H^{\pm}$) are predicted by several non-minimal Higgs scenarios, such as the Two Higgs Doublet Models (2HDM) [2] or models containing Higgs triplets [3]-[7]. As the Standard Model (SM) does not contain any elementary charged scalar particle, the observation of a charged Higgs boson would indicate physics beyond the SM. All analyses presented here [8]-[12] consider the type-II 2HDM, which is also the Higgs sector of the Minimal Supersymmetric Standard Model (MSSM). For charged Higgs boson masses $m_{H^{\pm}}$ smaller than the top-quark mass m_t, the dominant production mode at the LHC for $H^{\pm}$ is through top-quark decay via $t \to bH^+$, with the dominant source of top quarks being $t\bar{t}$ pair production.

2.1 Charged Higgs search with $H^+ \to \tau_{\text{lep}}\nu$ + lepton

A search for the charged Higgs boson in the decay channel $H^+ \to \tau_{\text{lep}}\nu$ [8] is presented here. The analysis is based on 1.03 fb^{-1} of data and relies on the detection of two light leptons (electron or muon) in $t\bar{t}$ events, where one charged lepton ℓ arises from the leptonically decaying τ lepton from $H^+ \to \tau_{\text{lep}}\nu$ while the other, oppositely charged, lepton arises from a leptonically decaying W boson. In the absence of a significant signal on top of the SM background, upper limits on the branching ratio $\mathscr{B}(t \to bH^+)$ are derived, under the assumption that $\mathscr{B}(H^+ \to \tau\nu) = 100\%$.

2.1.1 Event selection

The $\tau_{\text{lep}}\nu$+ lepton analysis requires exactly two oppositely charged leptons with at least one matched to the single-lepton trigger with thresholds low enough to guarantee the chosen leptons to be in the plateau region of the trigger-efficiency curve. At least four jets with $p_{\text{T}} > 20$ GeV are required, with exactly two of them being b-tagged. For ee and $\mu\mu$ events, cuts on the dilepton invariant mass are applied to veto Z bosons, together with a cut on the missing transverse energy $E_{\text{T}}^{\text{miss}}$. For $e\mu$ events, a cut on the scalar sum of the transverse energies of the two leptons and all selected jets is applied.

2.1.2 Reconstruction of discriminating variables

The identification of discriminating variables allows a distinction between leptons produced in $\tau_{\text{lep}} \to \ell\nu_\ell\nu_\tau$ decays and leptons from W boson decays.

One such discriminating variable is the invariant mass $m_{b\ell}$ of a b-quark and a light charged lepton ℓ coming from the same top quark, or more conveniently $\cos\theta_\ell^*$ [8], shown in Figure 1 (left). If a top-quark decay is mediated through an H^+ and if the H^+ is heavier than the W boson,

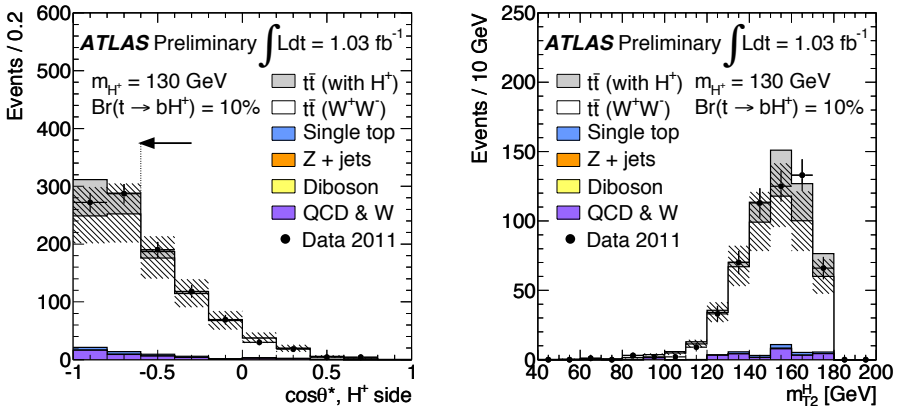

Figure 1: Reconstruction of $\cos\theta_\ell^*$ on the $t \to bH^+$ side of the dilepton events (left) and of the generalised transverse mass m_{T2}^H when $\cos\theta_\ell^* < -0.6$, in ATLAS data and Monte Carlo simulation. The striped area shows the systematic uncertainties for the SM backgrounds. The grey histogram shows the predicted contribution of events with a 130 GeV charged Higgs boson, assuming $\mathscr{B}(t \to bH^+) = 10\%$ and $\mathscr{B}(H^+ \to \tau\nu) = 100\%$. Taken from [8].

the b-quark usually has a smaller momentum than in the case of a W-mediated top-quark decay. Also a light charged lepton ℓ arising from a τ decay is likely to have a smaller momentum than a lepton coming directly from a real W boson. As a result, the presence of a charged Higgs boson in a leptonic quark decay leads to $\cos\theta_\ell^*$ values mostly close to -1. The signal region is chosen to be $\cos\theta_\ell^* < -0.6$. Another discriminating variable is the generalised charged Higgs boson transverse mass m_{T2}^H [10] and is shown in Figure 1 (right) for $\cos\theta_\ell^* < -0.6$. By construction, this transverse mass is larger than the true charged Higgs boson mass m_{H^+} and smaller than the top-quark mass. Therefore it can serve as a discriminant between top-quark decays mediated by a W or charged Higgs boson, based on their different masses. Neither an excess of events nor a significant deformation of the m_{T2}^H distribution is observed.

2.1.3 Results and limits

Since the data are found to agree well with the SM expectation, upper limits are put on the branching ratio $\mathscr{B}(t \to bH^+)$ as a function of the charged Higgs boson mass m_{H^+}, assuming $\mathscr{B}(H^+ \to \tau\nu) = 100\%$. Figure 2 shows the 95% confidence level (CL) upper limits on the branching ratio $\mathscr{B}(t \to bH^+)$.

2.2 Charged Higgs search with $H^+ \to \tau_{\text{lep}}\nu$ + jets

The search for a charged Higgs search with $H^+ \to \tau_{\text{lep}}\nu$ + jets [9] relies on the detection of $t\bar{t}$ events with a lepton ℓ (electron or muon) arising from the decay $H^+ \to \tau_{\text{lep}}\nu$ and jets arising from the hadronically decaying W boson. The search has been carried out using 4.6 fb^{-1} of pp collision data. In the absence of a significant signal, limits on the branching ratio $\mathscr{B}(t \to bH^+)$ are derived, assuming that $\mathscr{B}(H^+ \to \tau\nu) = 100\%$.

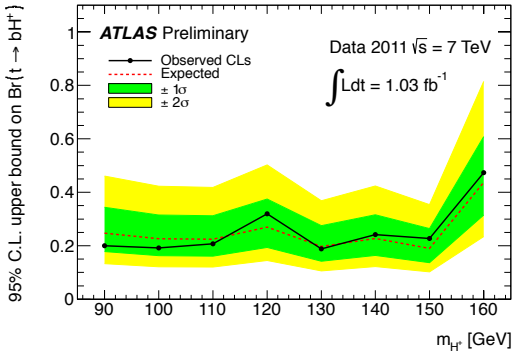

Figure 2: Upper limit on $\mathscr{B}(t \to bH^+)$ as a function of the charged Higgs boson mass, obtained for an integrated luminosity of 1.03 fb^{-1} and with the assumption that $\mathscr{B}(H^+ \to \tau\nu) = 100\%$ for the channel $H^+ \to \tau_{\text{lep}}\nu$ + lepton. All systematic uncertainties are included. The solid lines denote the observed 95% CL upper limits, while the dashed lines represent the expected limits. The outer edges of the green and yellow shaded regions show the 1σ and 2σ error bands. Taken from [8].

2.2.1 Event selection

The $\tau_{\text{lep}}\nu$+ jets analysis uses events passing a single-lepton trigger. To select a sample of $\tau_{\text{lep}}\nu$+ jets events enriched in $t\bar{t}$ pairs, additional requirements are made. Leptons are required to match the corresponding trigger object, with neither a second lepton nor a τ jet in the event, and pass a certain $E_{\text{T}}/p_{\text{T}}$ threshold depending on the flavour. At least four jets with $p_{\text{T}} > 20$ GeV with exactly two of them being b-tagged have to be present in the event. Requirements on the missing transverse energy $E_{\text{T}}^{\text{miss}}$ are also placed.

2.2.2 Reconstruction of discriminating variables

The analysis uses two variables that discriminate between leptons produced in $\tau_{\text{lep}} \to \ell\nu_\ell\nu_\tau$ and leptons coming directly from W boson decays.

The first variable is $\cos\theta_\ell^*$ [9], as in the $\tau_{\text{lep}}\nu$+ lepton analysis, see Section 2.1.2. The $\cos\theta_\ell^*$ distribution measured in the data, is shown in Figure 3 (left), superimposed on the predicted background, determined with a data-driven method for the multi-jet background and simulation for the other SM backgrounds [9]. The signal region is defined by requiring $\cos\theta_\ell^* < -0.6$ and a transverse W boson mass $m_{\text{T}}^W < 60$ GeV where

$$m_{\text{T}}^W = \sqrt{2p_{\text{T}}^\ell E_{\text{T}}^{\text{miss}}(1-\cos\Delta\phi_{\ell,\text{miss}})}. \tag{2.1}$$

This is done in order to suppress the background from events with a W boson decaying directly into an electron or a muon. For events in the signal region, the second discriminating variable used to search for charged Higgs bosons, the transverse mass m_{T}^H [10] is shown in Figure 3 (right). The data are found to be consistent with the SM prediction and no significant deformation of the m_{T}^H distribution is observed.

2.2.3 Results and limits

Assuming $\mathscr{B}(H^+ \to \tau\nu) = 100\%$, upper limits at 95% CL have been set on the branching ratio $\mathscr{B}(t \to bH^+)$ between 5% ($m_{H^+} = 90$ GeV) and 1% ($m_{H^+} = 160$ GeV) and are shown in Figure 4.

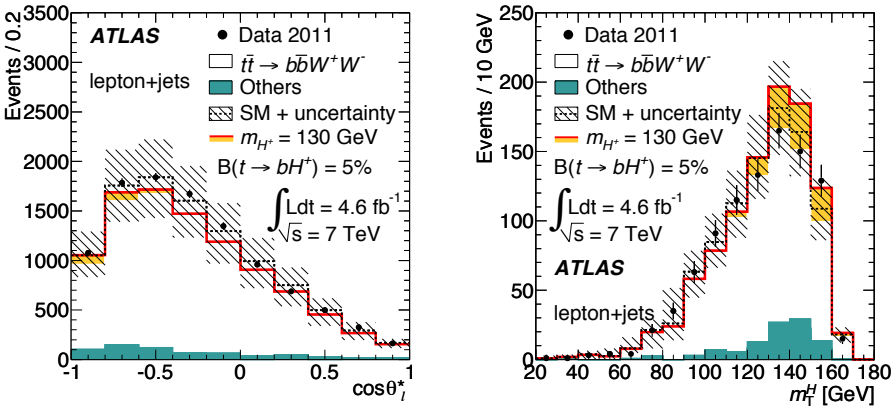

Figure 3: Distribution of $\cos\theta^*_\ell$ (left) and of the transverse mass m_T^H in the signal region $\cos\theta^*_\ell < -0.6$ and $m_{\mathrm{T}}^W < 60$ GeV in data and Monte Carlo simulation. The dashed line corresponds to the SM-only hypothesis and the hatched area around it shows the total uncertainty for the SM backgrounds where "Others" refers to the contribution of all SM processes except top-quark pair decays to $WbWb$. The solid line shows the predicted contribution of signal + background in the presence of a 130 GeV charged Higgs boson, assuming $\mathscr{B}(t \to bH^+) = 5\%$ and $\mathscr{B}(H^+ \to \tau\nu) = 100\%$. The light area below the solid line corresponds to the contribution of H^+ signal, stacked on top of the scaled $t\bar{t} \to bbWW$ background and other SM processes. Taken from [9].

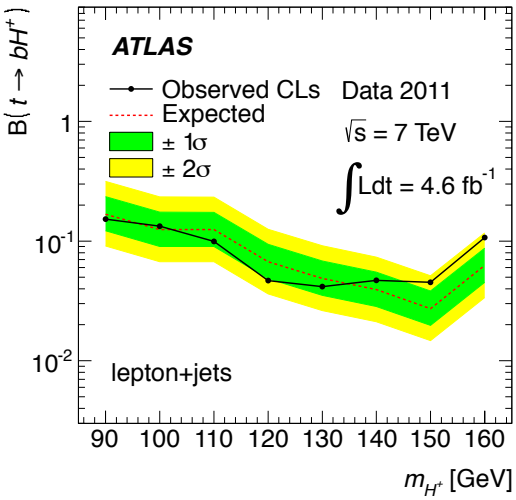

Figure 4: Observed and expected 95% CL exclusion limits on $\mathscr{B}(t \to bH^+)$ for charged Higgs boson production from top-quark decays as a function of m_{H^+}, assuming $\mathscr{B}(H^+ \to \tau\nu) = 100\%$, for the $\tau_{\mathrm{lep}}\nu$+jets channel. Taken from [9].

2.3 Charged Higgs search with $H^+ \to c\bar{s}$ + lepton

The search presented in this section is based on the semi-leptonic decay channel of $t\bar{t}$ candidates and uses the invariant mass distribution of two jets in the final state as a discriminating variable. In the absence of an excess of data with respect to the SM prediction, exclusion limits for $\mathscr{B}(t \to bH^+)$ are derived from early ATLAS data using 35 pb^{-1}, assuming that $\mathscr{B}(H^+ \to c\bar{s}) = 100\%$.

2.3.1 Event selection

Exactly one lepton with a high transverse momentum is required. To suppress backgrounds from multi-jet events, a minimum requirement is set on the missing transverse energy $E_{\mathrm{T}}^{\mathrm{miss}}$. Further reduction of the multi-jet background is achieved by cutting on the transverse mass m_{T} of the lepton and $E_{\mathrm{T}}^{\mathrm{miss}}$ for the electron channel and the sum of m_{T} and $E_{\mathrm{T}}^{\mathrm{miss}}$ for the muon channel. At least four jets with $p_{\mathrm{T}} > 20$ GeV are required, with at least one of them being b-tagged.

2.3.2 Kinematic fit

In lepton plus four jets events, the two jets originating from decays of H^+ need to be identified in order to reconstruct the mass of H^+ candidates. A kinematic fitter [11] is used to identify and reconstruct the mass of dijets from W/H^+ candidates, by full reconstruction of the $t\bar{t}$ system. In the kinematic fitter, the lepton, the missing transverse energy from the neutrino $E_{\mathrm{T}}^{\mathrm{miss}}$, and the four jets are assigned to the decay partons from the $t\bar{t}$ system. The best combination is found by minimising a χ^2 function [12] for each assignment of jets to quarks, where up to the five leading jets in p_{T} are considered as possible top-quark decay products. The different jet to quark assignments and the two neutrino solutions give 12 possible combinations for a 4 jet event, where one jet has been identified as originating from a b-quark. For 5 jet events, the two leading jets are always assumed to be top-quark decay products to reduce the combinatorics in the fit procedure. The combination with the smallest χ^2 value is selected. This selection has an efficiency of 82% for $t\bar{t}$ events.

2.3.3 Results and limits

The dijet mass distribution shown in Figure 5 is in good agreement with the expectation from SM and limits are set on the branching ratio $\mathscr{B}(t \to bH^+)$, assuming $\mathscr{B}(H^+ \to c\bar{s}) = 100\%$.

The observed limits shown in Figure 6 are within one standard deviation of the expected limits and range from 25% to 14% for m_{H^+} from 90 to 130 GeV. The sensitivity of the presented analysis is comparable to the limits obtained at the Tevatron, where datasets with 25 times the integrated luminosity were used.

3. Search for anomalous production of prompt like-sign muon pairs

Events containing two high-p_{T}, prompt, like-sign leptons are rarely produced in the SM, but occur with an enhanced rate in several models of new physics, for example supersymmetry [13], universal extra dimensions [14], left-right symmetric models [15]-[18], Higgs triplet models [19]-[21]. Most of these models would result in an excess of like-sign dimuons over the background with no distinct kinematic features in contrast with other particles. However, doubly charged Higgs

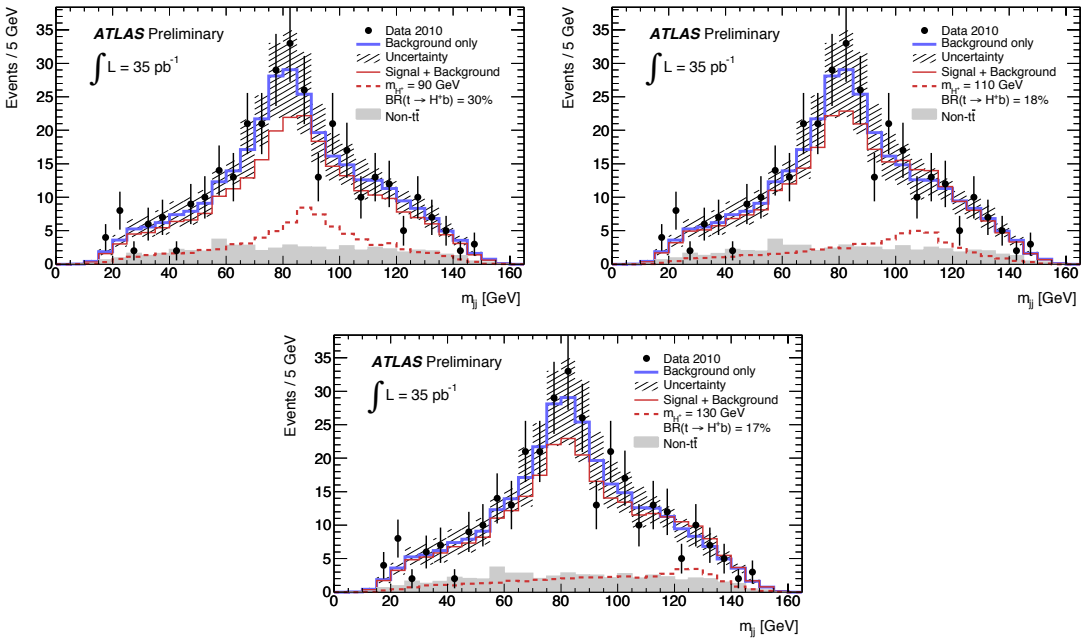

Figure 5: Dijet mass distribution of the data compared with the expectation from the SM or with simulated events where $\mathscr{B}(t \to bH^+) = 30\%$ ($m_{H^+} = 90$ GeV) (top left), $\mathscr{B}(t \to bH^+) = 18\%$ ($m_{H^+} = 110$ GeV) (top right) and $\mathscr{B}(t \to bH^+) = 17\%$ ($m_{H^+} = 130$ GeV) (bottom). The fractional uncertainty on the signal-plus-background model is comparable to the background-only model. Taken from [12].

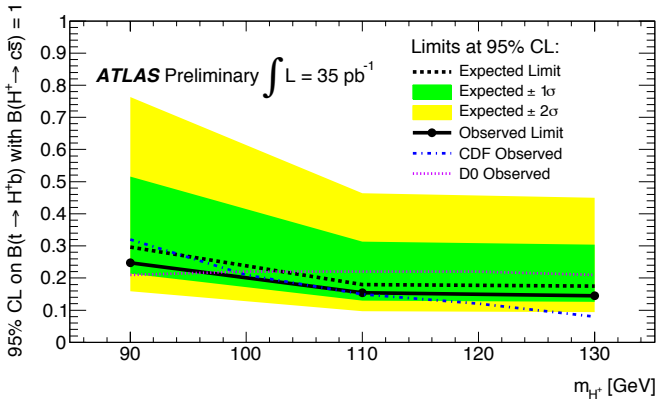

Figure 6: Observed 95% CL upper limit on $\mathscr{B}(t \to bH^+)$ compared with the expected results and limits from the Tevatron. The results assume $\mathscr{B}(H^+ \to c\bar{s}) = 100\%$. Taken from [12].

bosons ($H^{\pm\pm}$), predicted by some of these models, would be observed as a narrow resonance in the dimuon mass spectrum. In this analysis [22], events containing like-sign muon pairs are selected and their invariant mass distribution is compared to the SM prediction. Constraints on the $H^{\pm\pm}$ mass are placed as a function of its branching ratio to two muons. The inclusive search for anomalous production of two prompt, isolated muons with the same electric charge is performed in a data sample corresponding to 1.6 fb^{-1} of integrated luminosity.

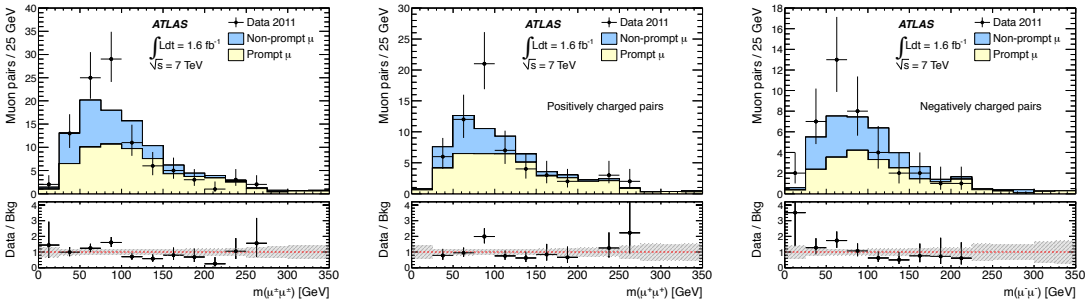

Figure 7: Distribution of the dimuon invariant mass for all $\mu^{\pm}\mu^{\pm}$ pairs (left), for positively charged $\mu^{+}\mu^{+}$ (middle) and negatively charged $\mu^{-}\mu^{-}$ pairs (right). The data are compared to the stacked background estimates. The ratio between the data and the predicted background is also shown, where the shaded region is the total systematic uncertainty on the background prediction. Taken from [22].

3.1 Event selection

Events are selected with an inclusive single-muon trigger. They must further contain at least two muons of the same electric charge satisfying a minimum p_{T} requirement and be within the acceptance of the tracking detector. Any combination of two muons is considered, allowing more than one muon pair per event to be included. A minimum cut on the mass of the two muons is required to exclude the low-mass hadronic resonances such as the J/Ψ and Υ mesons.

3.2 Comparison of the data to the background expectation

The SM backgrounds for like-sign dimuon final states can be divided into background from production of prompt like-sign dimuons, background caused by muons from hadronic decays (non-promt muons), and background from processes with two prompt opposite-sign muons where the charge of one of these muons is mismeasured. The simulation and determination of the various background contributions is described in [22].

The invariant mass distributions observed in the data are compared to the predicted background for $\mu^{\pm}\mu^{\pm}$, $\mu^{+}\mu^{+}$ and $\mu^{-}\mu^{-}$ production in Figure 7. The data agree with the SM prediction within the systematic uncertainties [22], and no excess is observed. The number of data events in the high-mass bins is lower than the background expectation, but in all mass bins the probability that the background gives a fluctuation as low or lower than observed in the data are found to be greater than 5%. In all mass bins, prompt muons from diboson production are the dominant background but non-prompt muons also contribute significantly: about 40% at low mass and 10% at high mass.

3.3 Results and limits

The expected and observed upper limits at 95% CL on the cross section times branching ratio, $\sigma(pp \to H^{++}H^{--}) \times \mathscr{B}(H^{\pm\pm} \to \mu^{\pm\pm}\mu^{\pm\pm})$ are shown in Figure 8. The observed upper limit is 11 fb at $m_{H^{\pm\pm}} = 100$ GeV and 1.7 fb at $m_{H^{\pm\pm}} = 400$ GeV. The median expected upper limits based on the background expectation together with the $\pm 1\sigma$ and $\pm 2\sigma$ uncertainty bands are also shown. The results derived from data are consistent with the expectation for the full mass range. The observed and expected limits on the mass of doubly charged Higgs bosons are also determined

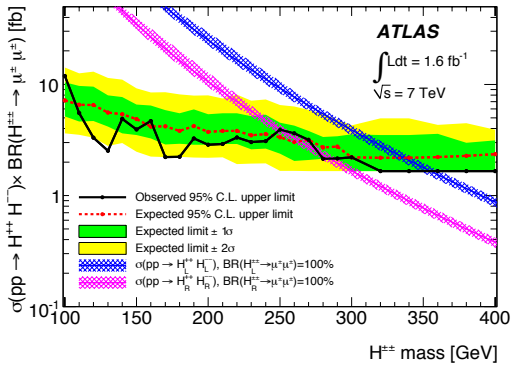

Figure 8: Observed and expected upper limit at 95% CL on the cross section times branching ratio for pair production of doubly charged Higgs boson decaying to two muons. Superimposed is the predicted cross section for $H_R^{++}H_R^{--}$ and $H_L^{++}H_L^{--}$ production assuming a branching ratio to muons of 100%. The bands on the predicted cross sections corresponds to the theoretical uncertainty of 10%. Taken from [22].

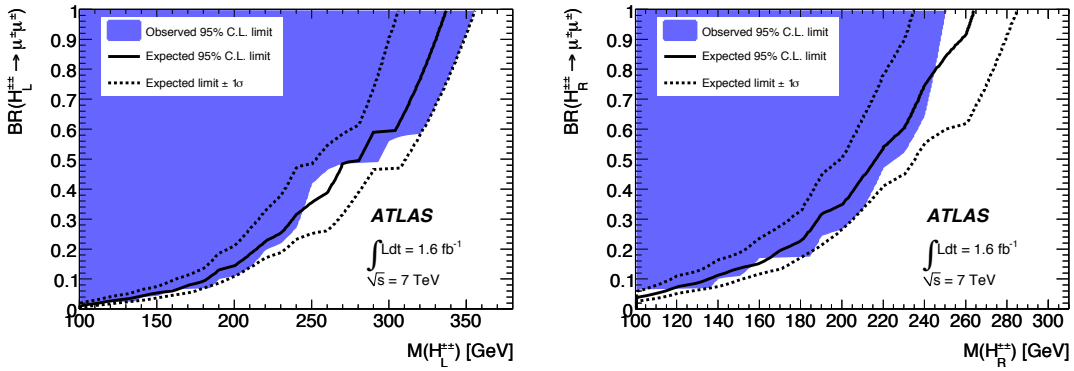

Figure 9: Exclusion region at 95% CL of the $H^{\pm\pm}$ mass as a function of the branching ratio to muon pairs $\mathscr{B}(H^{\pm\pm} \to \mu^{\pm}\mu^{\pm})$ for $H_L^{\pm\pm}$ bosons (left) and $H_R^{\pm\pm}$ bosons (right). The shaded areas show the observed exclusion region, the solid lines show the expected exclusion region, and the dashed lines show the $\pm 1\sigma$ variations of the expected exclusion region. Taken from [22].

as a function of the branching ratio to $\mu^{\pm\pm}\mu^{\pm\pm}$ assuming the central value of the theoretical cross section prediction. This is shown in Figure 9 for left- and right-handed Higgs bosons[1], respectively.

4. Conclusion

Charged and doubly charged Higgs bosons have been searched for in four different final states with pp collision data at $\sqrt{s} = 7$ TeV, recorded in 2010 and 2011 with the ATLAS experiment [1] at the LHC. In all four searches the observed data are found to be in agreement with the SM prediction, therefore upper limits at the 95% CL have been set on $\mathscr{B}(t \to bH^{+})$ and $\mathscr{B}(H^{\pm\pm} \to \mu^{\pm}\mu^{\pm})$.

[1]Doubly charged Higgs bosons couple to Higgs, electroweak gauge bosons and either left-handed or right-handed charged leptons. They are denoted $H_L^{\pm\pm}$ and $H_R^{\pm\pm}$, respectively.

References

[1] ATLAS Collaboration, 2008 JINST **3** S08003.

[2] T. Lee, Phys. Rev. D **8** (1973) 1226.

[3] T. P. Cheng and L. F. Li, Phys. Rev. D **22** (1980) 2860.

[4] J. Schechter and J. W. F. Valle, Phys. Rev. D **22** (1980) 2227.

[5] G. Lazarides, Q. Shafi and C. Wetterich, Nucl. Phys. B **181** (1981) 287.

[6] R. N. Mohapatra and G. Senjanovic, Phys. Rev. D **23** (1981) 185.

[7] M. Magg and C. Wetterich, Phys. Lett. B **94** (1980) 61.

[8] ATLAS Collaboration, ATLAS-CONF-2011-151, `https://cdsweb.cern.ch/record/1398187`.

[9] ATLAS Collaboration, JHEP **1206** (2012) 039 [arXiv:1204.2760 [hep-ex]].

[10] E. Gross and O. Vitells, Phys. Rev. D **81** (2010) 055010, [arXiv:0907.5367].

[11] CDF Collaboration, Phys. Rev. Lett. **103**, 101803 (2009).

[12] ATLAS Collaboration, ATLAS-CONF-2011-094, `http://cdsweb.cern.ch/record/1367737`.

[13] R. M. Barnett, J. Gunion, and H. Haber, Phys. Lett. B **315**, 349 (1993).

[14] J. Alwall, P. Schuster, and N. Toro, Phys. Rev. D **79**, 075020 (2009).

[15] J. C. Pati and A. Salam, Phys. Rev. D **10**, 275 (1974).

[16] R. N. Mohapatra and J. C. Pati, Phys. Rev. D **11**, 566 (1975).

[17] G. Senjanovic and R.N. Mohapatra, Phys. Rev. D **12**, 1502 (1975).

[18] T. Rizzo, Phys. Rev. D **25**, 1355 (1982); 27, 657 (1983).

[19] J. E. Cieza Montalvo, N. V. Cortez, J. Sa Borges, and M. D. Tonasse, Nucl. Phys. B **756**, 1 (2006); B **796**, 422(E) (2008).

[20] H. Georgi and M. Machacek, Nucl. Phys. B **262**, 463 (1985).

[21] J.F. Gunion, R. Vega, and J. Wudka, Phys. Rev. D **42**, 1673 (1990).

[22] ATLAS Collaboration, Phys. Rev. D **85** (2012) 032004 [arXiv:1201.1091 [hep-ex]].